Vol 17 No 4, April 2008
1674-1056/2008/17(04)/1341-08

Chinese Physics B

© 2008 Chin. Phys. Soc.
and IOP Publishing Ltd

Mean-field potential calculations of high-pressure equation of state for BeO*

Zhang Qi-Li(张其黎)†, Zhang Ping(张 平),
Song Hai-Feng(宋海峰), and Liu Hai-Feng(刘海风)

Institute of Applied Physics and Computational Mathematics, Beijing 100088, *China*

(Received 18 June 2007; revised manuscript received 2 November 2007)

A systematic study of the Hugoniot equation of state, phase transition, and the other thermodynamic properties including the Hugoniot temperature, the electronic and ionic heat capacities, and the Grüneisen parameter for shock-compressed BeO, has been carried out by calculating the total free energy. The method of calculations combines first-principles treatment for 0 K and finite-T electronic contribution and the mean-field-potential approach for the vibrational contribution of the lattice ion to the total energy. Our calculated Hugoniot is in good agreement with the experimental data.

Keywords: Hugoniot, mean-field-potential,first-principles
PACC: 6550, 6430, 7115

1. Introduction

As one member of the series of alkaline–earth oxides, beryllium oxide (BeO) has many unique properties. First, it is the only one of the alkaline–earth oxides to crystallize in the wurtzite (WZ) rather than the rock-salt (RS) structure. Furthermore, not only is BeO harder than the other alkaline–earth oxides but also it is among the hardest materials known. It is a good insulator like other alkaline–earth oxides, but its heat conductivity is an order of magnitude higher, which makes it a technically promising ceramic.[1] Also, BeO has a high melting point. These interesting physical properties are related to the characteristic features of interatomic bonding in BeO: for example, Compton scattering measurements revealed a significant component of the primarily ionic bonding in BeO.[2]

An important issue for BeO is its pressure-induced phase transition sequence, which has been investigated in a few experimental[3,4] and theoretical studies.[5−9] This is motivated by the well-known dielectric theory of Phillips and Van Vechten[10] that the structural phase stabilities of the $A^N B^{8-N}$ compounds can be related to their ambient spectroscopic ionicities (f_i). According to this theory, binary compounds with $f_i > 0.785$ will crystallize in a sixfold coordinated structure such as RS, while those with $f_i < 0.785$ crystallize in a fourfold structure such as zincblende (ZB) or wurtzite (WZ). BeO has a Phillips ionicity[10] of 0.602 and crystallize in the WZ structure under ambient conditions, in accord with the dielectric theory. Under pressure, the dielectric theory[10] predicts that the tetragonal compounds with $f_i > 0.35$ first transform to an ionic sixfold structure and then to some metallic phase, while those with $f_i < 0.35$ transforms to the metallic phase directly. With this understanding, however, the pressure-induced phase sequence for BeO is not yet fully understood. The early two *ab initio* calculations support this general prediction that a WZ→RS transition occurs at 22 GPa[5] (40 GPa in Ref.[4]). On the other hand, the latter calculations predicted the WZ first transformed into zinc blende (ZB) and then into RS. Herein, the work of Van Camp and Van Doren using soft nonlocal pseudopotential predicted the WZ-ZB-RS transitions at 74 and 137 GPa,[11] while Park *et al*,[12] who used a first-principles soft nonlocal pseudopotential method within the generalized-gradient approximation (GGA), predicted the transition pressure to be 91 (WZ→ZB) and 147 GPa (ZB→RS). This unusual transition sequence is attributed to the large charge asymmetry and the small bond length of BeO.[12] By use of full-potential linear muffin-tin or-

*Project supported in part by the National Natural Science Foundation of China (Grant Nos 10544004 and 10604010).
†E-mail: zhang_qili@iapcm.ac.cn

bital (FPLMTO) method, Boettger and Wills[9] have also predicted a WZ→ZB→RS phase transition sequence with the final transition at about 95 GPa. They also predicted a theoretical Hugoniot, consistent with shock wave data up to 100 GPa. More recently, Cai *et al*,[13] by systematically calculating the enthalpy barrier of the phase transition, have shown that only the WZ→RS transition will occur with increasing pressure.

Experimentally, Raman spectra showed no evidence for a phase transition at pressures up to 55 GPa in BeO[4] and Hugoniot data did not reveal any volume change for stresses up to 100 GPa.[4] The most recent static high pressure x-ray diffraction experiment[14] also showed no phase transition up to 126 GPa, but a new phase was found at 137 GPa. With increasing pressure, the WZ phase disappeared at 175 GPa.[14]

In this paper we theoretically study the phase transformation and Hugoniot of BeO under shock-wave dynamic compression, which is one of the most efficient ways to explore the thermodynamic properties of a material at ultrahigh pressures and temperatures. From its derived Hugoniot state one can deduce much useful information such as equation of state (EOS) in a feasible temperature range. The theoretical method we employed in this paper is a combined *ab initio* electronic structure calculation and classical mean-field potential (MFP) thermodynamic treatment.[15] Recent efforts have applied the MFP approach to a number of prototype metals,[15,16] indicating that both the calculated Hugoniot equation of state (at pressures up to ∼1000 GPa and temperatures up to ∼70000 K) and room temperature isotherms are well defined within the experimental uncertainties. We calculate the 0 K enthalpies of WZ, ZB, and RS BeO as functions of pressure. The results show that the enthalpy of WZ BeO is equal to that of ZB BeO at 84 GPa. When the pressure is increased to 105 GPa, the enthalpies of WZ and RS BeO come to cross each other. Based on our first-principles total energy data, we give a MFP analysis of the phase transition, Hugoniot EOS and the other thermodynamic properties for shock-compressed BeO. Our calculated Gibbs free energies show that the WZ→RS transition pressure is 103.8 GPa. Furthermore, our calculated Hugoniot is in good agreement with the experimental data.

2. The method

For a system with a given averaged molecular volume V and the temperature T, the Helmholtz free-energy $F(V,T)$ per atom can be written as

$$F(V,T) = E_{\rm c}(V) + F_{\rm ion}(V,T) + F_{\rm el}(V,T), \qquad (1)$$

where $E_{\rm c}$ represents the 0 K total energy per molecule which is obtained from *ab initio* electronic structure calculation, $F_{\rm el}$ is the free energy due to the thermal excitation of electrons, and $F_{\rm ion}$ is the ionic vibrational free energy evaluated from the partition function $Z_{\rm ion} = \exp(-NF_{\rm ion}/k_{\rm B}T)$. Here N is the total number of lattice ions. In the mean-field approximation, the classical $Z_{\rm ion}$ is given by[17]

$$Z_{\rm ion} = \left(\frac{mk_{\rm B}T}{2\pi\hbar^2}\right)^{3N/2} \times \left(\int \exp\left(-g(r,V)/k_{\rm B}T\right){\rm d}r\right)^N. \qquad (2)$$

The essential of the MFP approach is that the mean-field potential $g(r,V)$ is simply constructed in terms of $E_{\rm c}$ as follows:[15]

$$g(r,V) = \frac{1}{2}\left[E_{\rm c}(R+r) + E_{\rm c}(R-r) - 2E_{\rm c}(R)\right], \qquad (3)$$

where r represents the distance at which the lattice ion deviates from its equilibrium position R. It should be mentioned that the well-known Dugdale–MacDonald expression[18] for the Grüneisen parameter can be derived by expanding $g(r,V)$ to the order r^2. Then, $F_{\rm ion}$ can be formulated as

$$F_{\rm ion}(V,T) = -k_{\rm B}T\left(\frac{3}{2}\ln\frac{mk_{\rm B}T}{2\pi\hbar^2} + \ln v_{\rm f}(V,T)\right), \qquad (4)$$

with

$$v_{\rm f}(V,T) = 4\pi\int \exp\left(-\frac{g(r,V)}{k_{\rm B}T}\right) r^2{\rm d}r. \qquad (5)$$

When the electron-phonon interaction and the magnetic contribution are neglected, the electronic contribution to the free energy is $F_{\rm el} = E_{\rm el} - TS_{\rm el}$, where the bare electronic entropy $S_{\rm el}$ takes the form[19]

$$S_{\rm el}(V,T) = -k_{\rm B}\int n(\epsilon,V)[f\ln f + (1-f) \times \ln(1-f)]{\rm d}\epsilon, \qquad (6)$$

where $n(\epsilon, V)$ is the electronic density of states and f is the Fermi distribution. By using Eq.(6), the energy $E_{\rm el}$ due to electron excitations can be expressed as

$$E_{\rm el}(V,T) = \int n(\epsilon,V) f \epsilon {\rm d}\epsilon - \int^{\epsilon_{\rm F}} n(\epsilon,V)\epsilon {\rm d}\epsilon, \quad (7)$$

where $\epsilon_{\rm F}$ is the Fermi energy. In Fig.1 we show the $F_{\rm el}$ and $F_{\rm ion}$ for WZ structure at 2000 K plotted as functions of volume . It can be seen that the ionic vibrational free energy $F_{\rm ion}$ is larger than the electronic contribution to the free energy $F_{\rm el}$ in the whole volume range at 2000 K, and the difference between these two kinds of contribution is growing with the volume. Given the Helmholtz free-energy $F(V,T)$, the other thermodynamic functions such as the entropy $S = -(\partial F/\partial T)_V$, the internal energy $E = F + TS$, the pressure $P = -(\partial F/\partial V)_T$, and the Gibbs free energy $G = F + PV$, can be readily calculated.

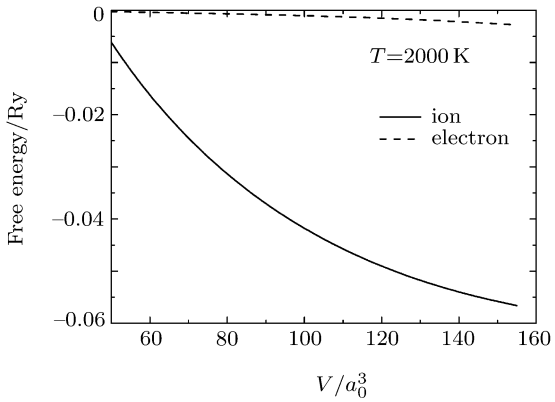


Fig.1. Calculated $F_{\rm el}$ and $F_{\rm ion}$ for WZ structure at 2000 K, as functions of volume, a_0 is the Bohr radius.

3. Results and discussion

First we calculate the 0 K total energy $E_{\rm c}(V)$ in a wide range of volumes. For this we employ the full-potential linearized-augmented-plane-wave (FPLAPW) method[20] within GGA.[21] The total energy of WZ structure BeO is calculated for 96 lattice constants ranging from 4.14 a.u. (1a.u.=0.0529177 nm) to 6.04 a.u. in steps of 0.02 a.u., while for the ZB structure BeO 91 lattice constants are considered ranging from 6.22 a.u. to 8.02 a.u. in steps of 0.02 a.u.. Finally for RS BeO we sample 81 lattice constants ranging from 5.46 a.u. to 8.66 a.u. in steps of 0.04 a.u.. As a reference, we mention that the calculated zero-pressure lattice constants for the three BeO structures are $a = 5.135$ a.u. ($c/a = 1.623$, WZ), 7.232 a.u. (ZB), and 6.894 a.u. (RS). In all of the three structures of BeO and for all the atomic volumes considered, we use the constant value of the muffin-tin radii $R_{\rm mt}$ of 1.2 a.u. for Be atom and 1.0 a.u. for O atom . The plane-wave cutoff $K_{\rm cut}$ is determined by $R_{\rm mt} \times K_{\rm cut} = 10.0$. Four thousands of k-points in the full Brillouin zone are used for reciprocal-space integrations. For the highest calculated pressure the atomic volume has exceeded the touching sphere limit, thus an extrapolation for gaining the 0 K total energy points by Morse function has been done.

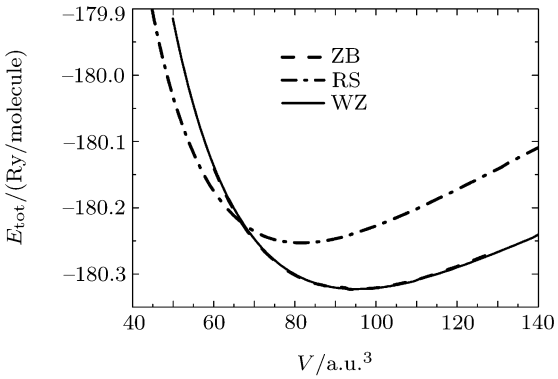


Fig.2. Calculated total energies for WZ, ZB, and RS phases of BeO as functions of volume.

Figure 2 shows the calculated 0 K total energies as functions of volume for WZ, ZB, and RS phases of BeO. The equilibrium volumes (per BeO molecule) corresponding to the minima in total energy are 95.53 a.u.^{3} (WZ), 95.02 a.u.^{3} (ZB), and 82.18 a.u.^{3} (RS). The equilibrium properties, including lattice parameters, bulk modulus from the fitting with Murnaghan curve,[22] and the equilibrium elastic constants for the three crystal structures of BeO, are listed in Table 1. For comparison, the available experimental data are also given in Table 1. The other available theoretical data have been collected in Ref.[2]. For WZ phase, the calculated equilibrium lattice constant and bulk modulus are 5.125 a.u. and 203 GPa, in good agreement with the experimental values of 5.098 a.u. and 212 GPa.[3] Also one can see that the calculated values of elastic constants c_{ij} for WZ structure agree with the measured data.

Table 1. Calculated and experimental structural parameters for WZ, ZB, and RS phases of BeO: equilibrium lattice constants a (a.u.), bulk modulus B_0 (GPa), and the elastic constants c_{ij} (GPa). Note that the c/a ratio for the WZ has been fully optimized.

Phase	a	c/a	B_0	c_{11}	c_{12}	c_{13}	c_{33}	c_{44}	c_{66}
WZ	5.125	1.623	203	432	120	87	463	142	156
WZ (exp.[a])	5.098	1.622	212	460	125	82	490	145	167
ZB	7.228	–	201	342	148	–	–	208	–
RS	6.894	–	231	298	214	–	–	294	–

[a]Reference [23].

To obtain the most stable structure at finite pressure and temperature, the Gibbs free energy $G = E + PV - TS$ should be used. For the experimental data, the last term is assumed small and therefore usually neglected by the previous theoretical studies.[5–9] For comparison with those calculations, we also work with the enthalpy $H = E + PV$ for each phase as the first step. The enthalpies of BeO with WZ, ZB, and RS structures are calculated, and the phase transition pressure is obtained from the enthalpy curve crossings. The difference in enthalpies between WZ and ZB types of BeO as functions of pressure are plotted in Fig.3, which shows that the two structures are energetically very close with the enthalpy difference typically of ∼5 meV in a wide range of pressures. This result is not surprising in view of the high similarity between the two structures. The local environment of any atom in either ZB or WZ phase is exactly the same as that of the second neighbours. One can see from Fig.3 that the enthalpy of WZ BeO is lower than that of ZB phase up to 84 GPa of pressure, while the enthalpy of ZB BeO begins to be lower for $P > 84$ GPa. It thus seems that the zero temperature WZ→ZB transition pressure is 84 GPa. This result is close to that (87 GPa) obtained by Cai *et al* [13] based on pseudopotential method with GGA. From the point of view of enthalpy barrier, however, Cai *et al* noticed that the WZ→ZB phase transition cannot happen up to 200 GPa. Here we adopt this point and will not consider the WZ→ZB transition in the following Hugoniot calculations.

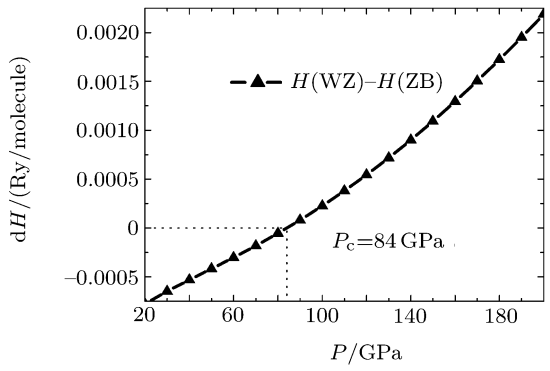


Fig.3. Calculated enthalpy difference between WZ and ZB types of BeO at 0 K as a function of pressure.

The enthalpies of BeO with WZ and RS structures are shown in Fig.4 as functions of pressure. One can see that the enthalpies of the two structures increase almost linearly with increasing pressure. When the pressure is up to 105 GPa they become equal. With further increasing pressure the RS structure becomes more stable. Thus it is expected to undergo a WZ→RS phase transition around P=105 GPa. This value is identical to that obtained in Ref.[13] but prominently differs from the calculated result of 147 GPa in Ref.[12]. This difference seems to be mainly caused by the different methods for finding the transition pressure.

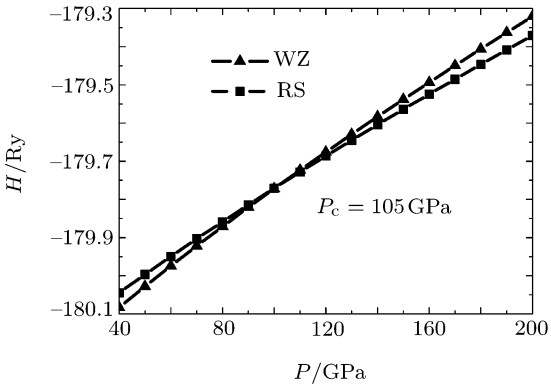


Fig.4. Calculated enthalpies of WZ and RS types of BeO at 0 K as functions of pressure.

Next we investigate the phase transition properties of BeO under shock-wave compression. In this case, we fully take into account the temperature effect in MFP framework and calculate the Gibbs free energies G of the Hugoniot states for the WZ and RS structures separately. Figure 5 shows the Gibbs free energies of these two structures as functions of the Hugoniot pressure. It can be seen that the overall

slope and the dependence of Gibbs free energy upon pressure for the two structures are essentially the same as those in zero-temperature case (Fig.4). The Hugoniot WZ→RS transition pressure is 103.8 GPa. Compared to zero-temperature result (105 GPa), one can see that the temperature effect (typically of 1000 K, see Fig.8 below) is small for WZ→RS phase transition in BeO. Thus we can draw a conclusion that the enthalpy can be reasonably used to study the phase transition of BeO in experimentally relevant temperature region. This is not surprising on considering the fact of high melting point of BeO.

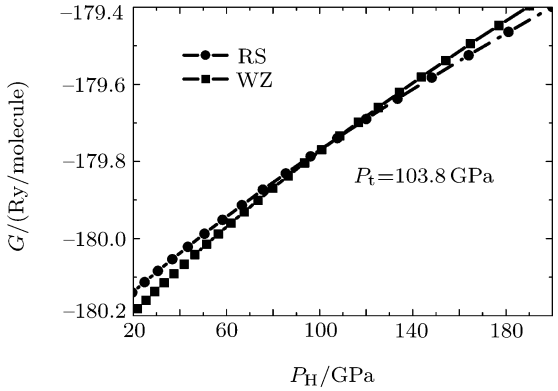


Fig.5. Calculated Gibbs free energies of the WZ and RS type BeO as functions of the Hugoniot pressure.

Now we turn to study the Hugoniot for BeO. Hugoniot states, which are derived by the conventional shock-wave technique,[23−27] are characterized by using measurements of shock velocity (U_s) and particle velocity (U_p) with $V_H/V_0 = (U_s - U_p)/U_s$ and $P_H = \rho_0 U_s U_p$, where P_H is the Hugoniot pressure, and ρ_0 is the initial density. By applying the Rankine–Hugoniot jump conditions, these data define a compression curve (volume V_H versus pressure P_H) as a function of known Hugoniot energy (E_H),

$$P_H(V_0 - V) = 2(E_H - E_0), \tag{8}$$

where V_0 and E_0 refer to the atomic volume and energy under ambient condition, respectively.

Unlike the static EOS, the temperature along the Hugoniot can vary in a range from room temperature to several tens of thousands of degrees, and thus the calculations of the Hugoniot state could serve as a good check of a theoretical method for the thermodynamic calculations. Using the calculated V_0 and E_0, we calculate the Hugoniot EOS for BeO at pressures up to 200 GPa. Due to the fact revealed in Fig.5 that there occurs a WZ→RS phase transition at the Hugoniot pressure $P_t = 103.8$ GPa, during the calculation of Hugoniot EOS, we take BeO structure as WZ for Hugoniot pressure $P_H < P_t$, while for $P_H > P_t$ the RS phase of BeO is taken. Correspondingly, the initial ambient volume (V_0) and energy (E_0) of WZ phase is used when $P_H < P_t$, while for $P_H > P_t$, the values of V_0 and E_0 refer to the RS phase. Our calculated Hugoniot EOS is shown in Fig.6 (solid curve) in the form of Hugoniot pressure (P_H) versus V_0/V. Note that to reproduce the experimental density,[3] in accord with the convention, here the 0 K isotherm of WZ structure is uniformly adjusted by reducing 5.85 GPa from each pressure and the energies are subsequently modified in a consistent fashion. For comparison with our theoretical results, the experimental data[18] are also shown in the figure (squares). One can see that an overall agreement between our calculated results and the experimental data is fairly good up to the experimentally reachable Hugoniot pressure of 102 GPa, except for four points in the range of 0–30 GPa where the strength effects are large. At present, unfortunately, no experimental shock-wave data at higher compression ($P_H > 102$ GPa) exist. Therefore, to verify our theoretical Hugoniot for RS phase at $P_H > P_t$ GPa, more experimental data are needed. However, based on the good agreement between our calculations and the experimental data available for WZ phase of BeO, and the coincidence between our calculated result of WZ–RS phase transition and the previous calculation,[13] we expect that our calculated Hugoniot curve of P_H versus V_0/V can be adopted in practical applications if the higher-pressure data are needed.

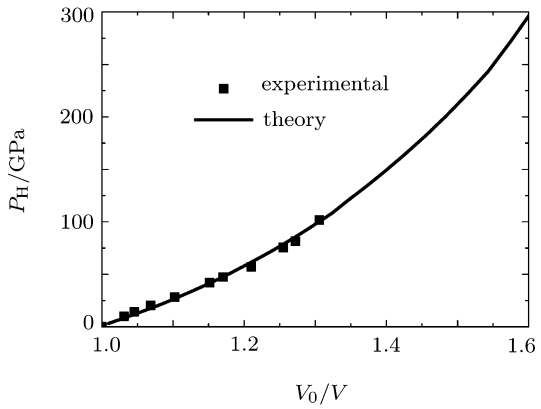


Fig.6. Calculated Hugoniot (solid line) in the form of Hugoniot pressure versus V_0/V plot and experimental data (squares)[18].

For further illustration, we have also transformed the calculated curve of $P_{\rm H}$ versus (V_0/V) to that of shock velocity $U_{\rm s}$ versus particle velocity $U_{\rm p}$. The result is plotted in Fig.7 (solid curve). The experimental data[3] are also shown in this figure (squares) for comparison. One can see that for moderate particle velocities (2km/s< $U_{\rm p}$ <3km/s), the calculated result agrees well with the experimental. Whereas for low particle velocities the discrepancy becomes apparent although the calculated starting point ($U_{\rm p}=0$) coincides exactly with the measurement (see Fig.7). Boettger *et al* have also noticed this discrepancy in their zero-temperature calculation.[9] This may be due to the experimental failure to correctly measure the particle velocity $U_{\rm p}$ in low shock-pressure region because of the presence of strength effect as mentioned above.

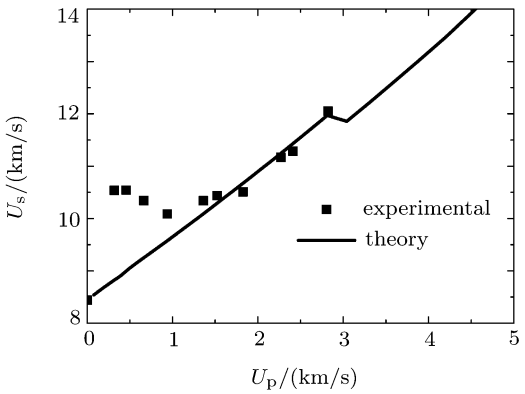


Fig.7. Calculated Hugoniot in the form of $U_{\rm s}$ versus $U_{\rm p}$ plot (solid line) and experimental data (squares)[18].

We also carried out the calculation of the temperature along the principal Hugoniot. Note that in the traditional treatment of the Hugoniot data, the temperature estimate remains less reliable since it requires the accurate knowledge of specific heat and the Grüneisen parameter values that are not well known. Using the present MFP, however, all these quantities can be calculated straightforward (see below). The calculated Hugoniot temperature is shown in Fig.8 as a function of pressure. During calculation, again, we take BeO structure as WZ for Hugoniot pressure $P_{\rm H} < P_{\rm t}$, while for $P_{\rm H} < P_{\rm t}$ the RS phase of BeO is chosen. The turning section around $P_{\rm t}$ in Fig.7 is due to this choice of different crystal phases in the two pressure regions separated by the transition point $P_{\rm H}=P_{\rm t}$. At present there is no experimental data of Hugoniot temperature available. Thus our calculated result needs to be verified in the future.

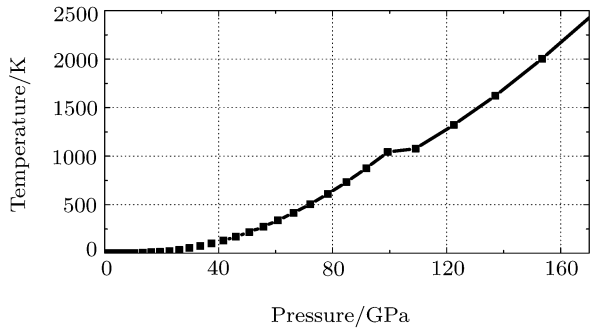


Fig.8. Calculated temperature along the principal Hugoniot for BeO. During calculation the crystal phase of BeO has been chosen to be wurtzite at pressures lower than WZ–RS transition point $P_{\rm t}$, and rocksalt for $P > P_{\rm t}$.

Since we have explicitly calculated the Helmholtz free energy $F(V,T)$ as a function of V and T, all other thermodynamic parameters can be calculated. In particular, one can evaluate the thermodynamic Grüneisen parameter. Given the isothermal bulk modulus B_T which is given by $B_T(V,T) = V\left(\dfrac{\partial^2 F}{\partial V^2}\right)_T$, the volume thermal-expansion coefficient $\beta_P(V,T) = \dfrac{1}{V}\left(\dfrac{\partial V(T)}{\partial T}\right)_P$, the constant-volume heat capacity $C_V = C_V^{\rm ion}(V,T) + \left(\dfrac{\partial E_{\rm el}(V,T)}{\partial T}\right)$, and the thermodynamic Grüneisen parameter can be obtained as follows:

$$\gamma_{\rm th} = \frac{V B_T(V,T)\beta_P(V,T)}{C_V(V,T)}. \tag{9}$$

Figure 9 plots our calculated $\gamma_{\rm th}V_0/V$ as a function of Hugoniot pressure $P_{\rm H}$. Again two crystal structures, i.e., the WZ phase for $P_{\rm H} < P_{\rm t}$ and the RS phase for $P_{\rm H} < P_{\rm t}$, are used in the calculation. One can see that the conventional assumption γ/V=constant for the treatment of shock-wave data is not applicable on the whole for the present case of BeO.

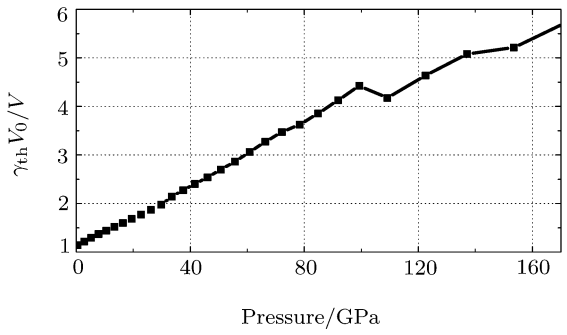


Fig.9. Calculated thermodynamic Grüneisen parameter along the principal Hugoniot for BeO. During calculation the crystal phase of BeO has been chosen to be wurtzite at pressures lower than WZ–RS transition point $P_{\rm t}$, and rocksalt for $P > P_{\rm t}$.

Figure 10 plots the constant-pressure heat capacity $C_{\rm P}$ which is calculated by

$$C_{\rm P}(V,T) = C_V(V,T) + VTB_T(V,T)\beta_P^2(V,T). \quad (10)$$

For comparison, the constant-volume heat capacity C_V and its ionic component $C_V^{\rm ion}$ are also shown in Fig.10. One can see that the thermal electronic contribution (the difference between the dashed line and the dotted line) to the heat capacity is negligibly small in a wide range of pressure. This is what one expects on considering the insulator nature of BeO. For metals, on the other hand, the thermal electronic contribution to C_V may be comparable to the lattice ion contribution at high compression due to the increasing electronic DOS at Fermi level.

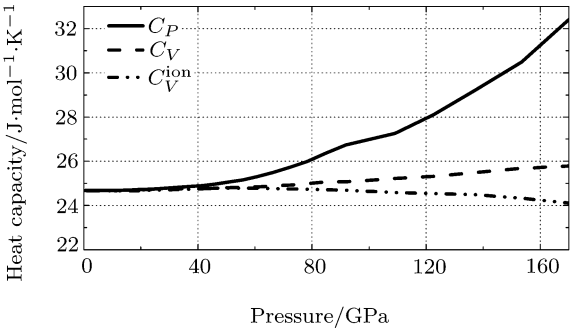


Fig.10. Calculated heat capacities along the principal Hugoniot for BeO. During calculation the crystal phase of BeO has been chosen to be wurtzite at pressures lower than WZ–RS transition point $P_{\rm t}$, and rocksalt for $P > P_{\rm t}$. The solid, dashed, and dotted curves represent the calculated constant-pressure specific heat C_P, constant-volume specific heat C_V, and the lattice ion only constant-volume $C_V^{\rm ion}$, respectively.

4. Summary

In summary, by using the first-principles FPLAPW total-energy calculation method combined with MFP treatment and taking into account the vibrational contribution of the lattice ions, we have systematically studied the Hugoniot EOS of shock-compressed BeO. Our calculated Hugoniot is in good agreement with the experimental data. The other thermodynamic properties, such as the Hugoniot temperature, the Grüneisen parameter, and the heat capacities including the ionic and electronic contributions, have also been calculated. In addition, the 0 K enthalpy and finite-temperature Gibbs free energies of BeO with WZ, ZB, and RS structures have also been calculated. These indicate that the variation of WZ→RS transition pressure with Hugoniot temperature is tiny. Therefore, the 0 K calculation is considerably reasonable in studying the solid-solid phase transition of BeO. We expect our present results may add some more understanding of the Hugoniot properties of oxides under shock-wave compression.

References

[1] Vidal-Valat G, Vidal J P, Kurki-Suonio K and Kurki-Suonio R 1987 *Acta Crystallogr.* A **43** 540

[2] Joshi K B, Jain R, Pandya R K, Ahuja B L and Sharma B K 1999 *J. Chem. Phys.* **111** 163

[3] Hazen R M and Finger L W 1973 *J. Appl. Phys.* **59** 3728
Marsh S P 1986 *High Pressures* **5** 503
also see 1980 *LASL Shock Hugoniot Data* Berkeley edited by March S P (University of California) p241

[4] Jephcoat A P, Hemley R J, Mao H K, Cohen R E and Mehl M J 1988 *Phys. Rev.* B **37** 4727

[5] Chang K J, Froyen S and Cohen M L 1983 *J. Phys.* C: *Solid State Phys.* **16** 3475

[6] Chang K J and Cohen M L 1984 *Solid State Commun.* **50** 487

[7] Lichanot A, Caillet M, Larrieu C, Dovesi R and Pisani C 1992 *Chem. Phys.* **164** 383

[8] Lichanot A and Rerat M 1993 *Chem. Phys. Lett.* **211** 249

[9] Boettger J C and Wills J M 1996 *Phys. Rev.* B **54** 8965

[10] Phillips J C 1973 *Bonds and Bands in Semiconductors* (New York: Academic)
Phillips J C 1970 *Rev. Mod. Phys.* **42** 317

[11] Van Camp P E and Van Doren V E 1996 *J. Phys.: Condens. Matter* **8** 3385

[12] Park C J, Lee S G, Ko Y J and Chang K J 1999 *Phys. Rev.* B **59** 13501

[13] Cai Y X, Wu S T, Xu R and Yu J 2006 *Phys. Rev.* B **73** 184104

[14] Mori Y, Ikai T and Takarabe K 2003 *Photon Factory Activity Report* **20(B)** 215

[15] Wang Y 2000 *Phys. Rev.* B **61** R11 863
Wang Y, Chen D Q and Zhang X W 2000 *Phys. Rev. Lett.* **84** 3220
Li L and Wang Y 2001 *Phys. Rev.* B **63** 245108
Wang Y, Ahuja R and Johansson B 2002 *J. Phys.: Condens. Matter* **14** 10895

[16] Song H F and Liu H F 2007 *Acta Phys. Sin.* **56** 2833 (in Chinese)

[17] Wasserman E, Stixrude L and Cohen R E 1996 *Phys. Rev.* B **53** 8296

[18] Dugdale J S and MacDonald D K C 1953 *Phys. Rev.* **89** 832

[19] Jarlborg T, Moroni E G and Grimvall G 1997 *Phys. Rev.* B **55** 1288

[20] Blaha P, Schwarz K, Madsen G, Kvasnicka D and Luitz J WIEN2K http://www.wien2k.at/

[21] Perdew P, Burke K and Ernzerhof M 1996 *Phys. Rev. Lett.* **77** 3865

[22] Murnaghan F D 1944 *Proc. Natl. Acad. Sci. USA* **50** 697

[23] *Los Alamos Shock Hugoniot Data* Berkeley 1980 edited by Marsh S P (University of California)

[24] Sirota N N, Kuzmina A M and Orlova N S 1990 *Dokl. Akad. Nauk SSSR* **314** 856

[25] Dai C D, Hu J B, Tan H and Yu Y Y 2005 *Acta Phys. Sin.* **54** 5750 (in Chinese)

[26] Jing F Q, Li X J, Wang F H and Yang C L 2000 *Acta Phys. Sin.* **49** 114 (in Chinese)

[27] Geng H Y, Tan H and Wu Q 2001 *Acta Phys. Sin.* **50** 1334 (in Chinese)